A Quadruple Active Bridge Converter as the Storage Interface in the More Electric Aircraft

Giampaolo Buticchi, Levy Costa, Davide Barater, Marco Liserre and Eugenio Dominguez

***Abstract*—The More Electric Aircraft (MEA) concepts aims at increasing the penetration of electric systems on the aircrafts. In this framework, the electrical power distribution system (EPDS) is of high importance. Increasing the electrical subsystem while limiting the overall weight is one of the major challenges for the MEA. This problem can be addressed by a proper energy storage system that allows increasing the utilization of the generators. This paper proposes the use of a Quadruple Active Bridge (QAB) converter, already adopted in other fields, to interfaces different storage technologies to the aircraft DC bus. This solution would replace multiple DC/DC converters, increasing the power density, but presents difficulty in the power flow control and in the possible efficiency deterioration in the case of asymmetrical operation. A novel control, based on current feed-forward and power decoupling is proposed to this aim and simulations shows the effectiveness of the solution. A laboratory prototype is used to confirm that the asymmetrical operation, where each port processes a different amount of power, does not imply a marked reduction of efficiency.**

I. Introduction

The more-electric aircraft (MEA) concept is one of the major trends in modern aerospace engineering aiming at the reduction of the overall aircraft weight, operation cost and environmental impact. Electrical systems are employed to replace existing hydraulic, pneumatic and mechanical actuators, guaranteeing the same or higher reliability levels [1]. As a consequence, the on-board installed electrical power increases significantly and this challenges the design of the aircraft electrical power distribution systems (EPDS). The typical installed capacity of the electrical system on an existing medium-range aircraft increased from 100 kW of a Boeing 737 to more the 1 MW of the more recent Boing 787 [2]. To withstand the increase of energy request, the size of electrical generators is increased as well. However, the choice of the nominal power of new generators is still an open research theme. In fact, if the generators were designed to match the maximum peak power value requested during the different flight phases, the advantages of weight reduction and fuel saving would be probably lost [3]. In this scenario, the distribution retains a significant role as an intelligent power management, that features different storage systems, could better exploit generation sources without necessarily increasing their rating. The correct dimensioning of the energy storage system has been investigated for some specific application [4] to identify the optimal trade-off between additional storage weight and fuel saving. A review of Emerging Energy Storage Solutions for Transportation was proposed in [5], focusing on different technologies of li-Ion batteries, fuel cells FC and ultracapacitors. These storage technologies have different properties, with regard to various attributes such as storage capacity, response time, power and cost. Therefore, it is impossible to specify a single energy storage solution that can satisfactorily fulfill the demands of a complex system such as an aircraft. The use of hybrid systems, adopting different technologies, is seen as the best solution for providing a better energy management and weight reduction for the MEA. One of the challenges in using hybrid energy systems is the development of interface electronics that allow an efficient exploitation of the different storage technologies.

A straightforward way to interface multiple storage technology is to employ multiple DC/DC power converters, like Dual Active Bridge (DAB), connected to the same DC bus. This solution allows a good individual power control of the different sources and the efficiency of the power electronics can be optimized for each power source. However, it presents an increased number of control boards, communication links, high frequency transformer and power stages, decreasing the power density. Since all energy sources are coupled to the same DC bus, a multi-port solution would help making the system more power dense, reducing the overall number of components.

This paper proposes a Quadruple Active Bridge (QAB) that interfaces a hybrid storage system that include FC, battery and UCs, to the EPDS of future aircraft. The open challenges with respect to a multi DAB solution are the prioritization of the different energy sources depending on the frequency content of the bus request and the possible efficiency drop when the converter is operating in a very asymmetrical way, i.e., one storage port is providing most of the power.

The paper is organized as follows, Section II reviews the EPDS architectures, Sections III and IV describe the QAB converter and its control. Section V and VI report the results. Finally, section VII draws the conclusion.

II. Electrical Power Distribution System

Each aircraft manufacturer adopts different Electrical Power Distribution Systems with mixed AC and DC bus. A number of different voltage standards exist for the electrical system on large civilian aircraft:

- 28 V DC - low power loads/avionics on large aircraft and complete electrical system on small aircraft.
- 270 V DC (bipolar $\pm 135V$) - military aircrafts and some subsystems on some larger aircrafts.
- 115 V AC at 400 Hz - larger loads on large civilian aircrafts.
- 540 V DC (bipolar $\pm 270V$).

978-1-5386-1180-7/18/$31.00 ©2018 IEEE

- 230 V AC at 400 Hz.

However, with MEA, the tendency is to replace traditional AC distribution and adopt only two main DC buses: a $\pm 270Vdc$ high voltage bus and a low 24 V dc bus mainly for avionics [2]. The AC sources are interfaced to the bus with AC/DC converters, the same for AC loads, such as electromechanical actuators, driven by DC/AC electric drives. This can increase efficiency, reduce weight and remove the need for reactive power compensation devices [6].

An example of EPDS for future regional aircrafts is shown in Fig. 1 where two main power generators and an auxiliary generator are connected to three independent bus bar that can work independently or connected together to enable power sharing between the generators. The system can also decide to exclude one bus bar in case of fault, reallocating the power between the generators. The low voltage buses include energy storage systems and in the scheme bidirectional DC/DC converters are used to exchange power between the High Voltage and Low Voltage buses. A Centralized Control Unit (CCU) synthesizes the best control strategy to manage the energy flow and supervise the functionalities of the DC/DC converters, deciding on-fly their operation in buck or boost mode.

During normal operation, the DC/DC converters are used in buck mode, charging the energy storage system if needed, but in case of emergency they can be used to supply critical high voltage loads. The choice of the best storage system is still under research, as fuel cells or battery are envisaged for their high energy density, whereas ultra/super capacitors can be included with the role of energy buffers, to help during high transient energy requests from electro mechanical actuators or other critical loads. However, the use of different kinds of storage poses issue that must be addressed by the EPDS. In fact, supercapacitors, batteries and/or fuel cells have different response times and an energy management system should feature a multi-scheme storage system, where depending on the optimization criteria (fuel consumption, life cycle maximization, stress of each component) different control schemes are activated.

Because of the reduced number of conversion stages and the intrinsically DC characteristics of the storage, this paper focuses on the DC solution for 270 V / 28 V EPDS. The technical challenges of this design are to guarantee a precise and fast control of the power processed by the different sources while still guaranteeing high efficiency, power density and galvanic isolation for safety purpose.

III. The Quadruple Active Bridge Converter

A multiple port converter based on active bridges was proposed in 2007 in [7]–[9] as a solution to interface multiple sources and still retain the galvanic isolation. The converter retains the basic characteristics regarding power transfer and soft switching as the Dual Active Bridge converter.

The schematic of the QAB if presented in Fig. 3. The adopted control is the phase-shift control, that implies that each full-bridge is driven with a 50% duty cycle and the shifting between the voltage square waves determines the power transfer.

Equation (1) describes the overall power that is processed by a single port, where n_{ij} is the turn ratio between the two ports, L_{ij} is the equivalent inductance from the two ports and d_{ij} is the phase shift angle normalized to 2π.

$$P_i = \sum_{j \neq i} \frac{n_{ij} V_i V_j}{L_{ij} f_{sw}} d_{ij} \left(1 - 2d_{ij}\right) \tag{1}$$

One of the challenges of the QAB is that the individual control of the single ports, because a modification of one phase-shift would lead to unbalancing the power processed by all other ports. In order to prevent this behavior, a decoupling mechanism must be implemented. The first step is to perform a linearization of equation (1), assuming that the inductance are designed to have the converter operating for small phase shift.

Linearizing the equations around the zero phase shift leads to the matrix A of equation (2), where it is seen that variation in the voltage (because of oscillations in the supercapacitors voltage or in the DC bus) and differences in the inductance must be taken into account for a proper compensation. Inverting the matrix and normalizing it to the nominal values of the inductance and voltage levels allows decoupling the power flow.

IV. Control description and tuning

The objective of the control is to ensure a stable bus regulation, prioritizing the fast storage during the transient and keeping the fuel cell power level as constant as possible. Fig. 4 shows the control, where a combination of High-Pass-Filter (HPF) and Low-Pass-Filter (LPF) allows selecting the different frequency components that are processed by each port. In addition, a current control for the battery should be implemented to control the state-of-charge (SOC) and a DC Link control for the average voltage of the supercapacitor.

The decoupling block can be implemented by inverting the matrix A in equation (2) and normalizing, like shown in equation (3).

$$\begin{pmatrix} d_{41} \\ d_{42} \\ d_{43} \end{pmatrix} = \frac{V_n}{L_{lk}} A^{-1} \begin{pmatrix} d_{fuelcell} \\ d_{batt} \\ d_{supercap} \end{pmatrix} \tag{3}$$

In order to study the control, a simplified model is shown in Fig. 5. The assumption is that, after the decoupling, the power flow of each port can be realized independently, as if the converter was composed of three separate DAB, whose phase shift controls the power exchange. The model is realized on an equivalent DAB with equal voltages at primary and secondary sides V_n, with a frequency f_{sw} and leakage inductance L_{lk}. In these conditions, $K_{eq} = 4\frac{V_n}{f_{sw} L_{lk}}$. The output of the voltage control regulator is d_{DC}, that is then divided into the high- and low-frequency components for the different sources. The load current is modeled as a voltage dependent generator, that can represent a resistor R_{load} or other loads, depending on

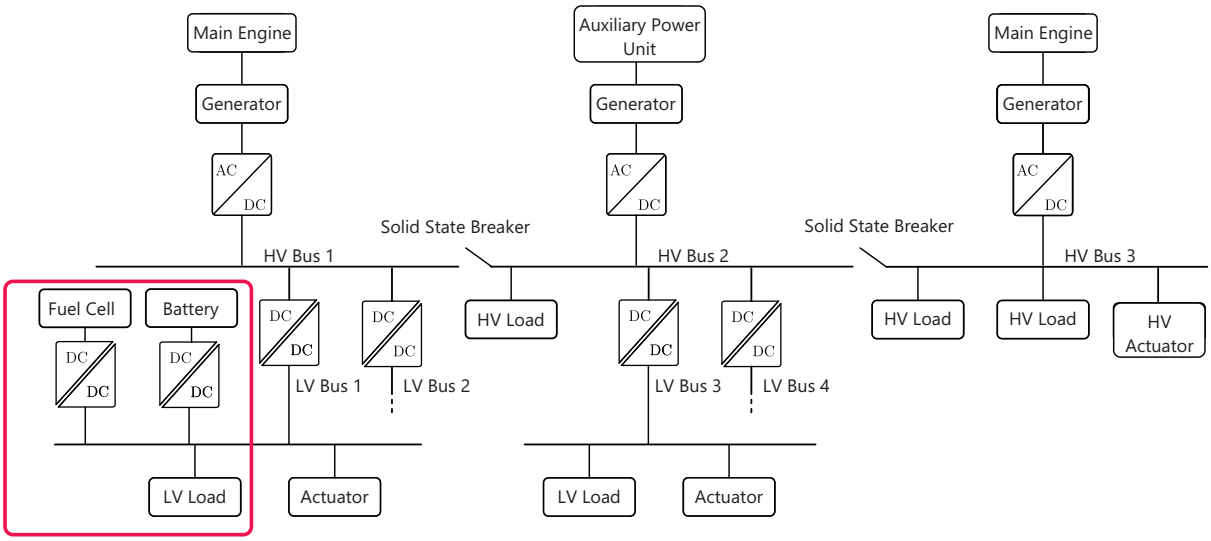

Fig. 1: Example of an electrical power distribution systems with the storage part highlighted.

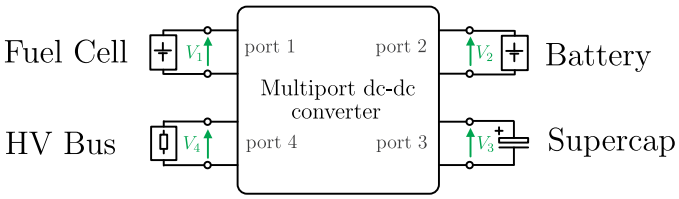

Fig. 2: Quadruple Active Bridge as a storage integration node connected to a DC bus.

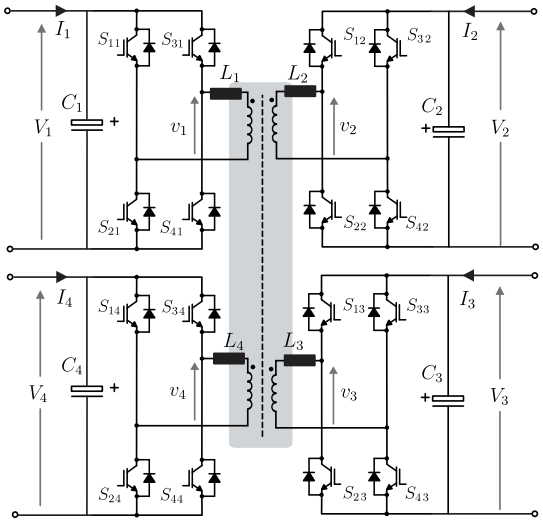

Fig. 3: Quadruple Active Bridge schematic.

the equipment (constant impedance, constant current, constant power).

For the initial controller tuning, only the capacitor equation is considered, and a PI controller is tuned to achieve a target crossover frequency with the maximization of the phase margin [10]. For the bus voltage control, a crossover frequency of 300 Hz is selected, while for the supercapacitor voltage control only 1 Hz is chosen. In fact, it is important the voltage control of the capacitor does not affect the system. Overvoltage or undervoltage of the capacitor can be prevented by saturating the phase shift.

The control realized with a simple PI regulator has a main drawback: the higher the phase margin of the design, the higher the output impedance becomes. As a consequence, fast-changing load will deteriorate the voltage regulation unless a very fast controller is realized. Moreover, the output of the PI regulator is limited by the chosen bandwidth, making impossible for the supercapacitor to follow rapid power variations. For this reason, a current feed forward is used to reduce the output impedance and bypass the PI regulator during fast load variations, as shown in Fig. 4. The same objective could have been realized by applying an impedance shaping technique, like in [11].

Fig. 6 shows the frequency responses of the voltage control and of the output impedance with the voltage control and with the current feed-forward. As can be seen, the current feed-forward allows for a better disturbance rejection. Nominal voltages of 28 V for all ports, switching frequency f_{sw} = 20 kHz, bus capacitance 0.5 mF and L_{lk} = 1 uH.

V. Simulations

The decoupling and feed-forward were tested in a Simulink environment with the aid of the PLECS toolbox. For each port, the voltage is 28 V and the rated current for the bus port is 90 A, this implies a total power of 2.5 kW. The rated normalized phase shift d_n is chosen equal to 0.1 (equivalent to 36 degrees), in order to have some control margin and to limit the reactive current between the ports [12]. When the QAB is operating at full power, i.e., all storage ports transfer the rated power to the bus, the three ports operate in parallel. In order to satisfy these requirements, a leakage inductance L_{lk} of 1 uH is chosen in the simulations. Because the operation of the converter is

$$\begin{pmatrix} P_1 \frac{f_{sw}}{n_1 V_1} \\ P_2 \frac{f_{sw}}{n_2 V_2} \\ P_3 \frac{f_{sw}}{n_3 V_3} \end{pmatrix} = \begin{pmatrix} \frac{V_4}{L_{14}} + \frac{V_2}{n_2 L_{12}} + \frac{V_3}{n_3 L_{13}} & -\frac{V_2}{n_2 L_{12}} & -\frac{V_3}{n_3 L_{13}} \\ -\frac{V_1}{n_1 L_{21}} & \frac{V_4}{L_{24}} + \frac{V_1}{n_1 L_{21}} + \frac{V_3}{n_3 L_{23}} & -\frac{V_3}{n_3 L_{23}} \\ -\frac{V_1}{n_1 L_{31}} & -\frac{V_2}{n_2 L_{32}} & \frac{V_4}{L_{34}} + \frac{V_1}{n_1 L_{31}} + \frac{V_2}{n_2 L_{32}} \end{pmatrix} \begin{pmatrix} d_{41} \\ d_{42} \\ d_{43} \end{pmatrix} = A\,[d] \qquad (2)$$

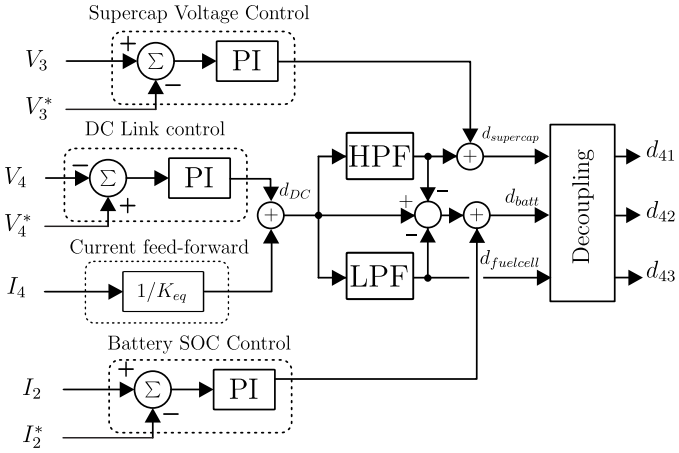

Fig. 4: Control of the QAB, including state-of-charge for the battery and voltage control for the supercapacitor.

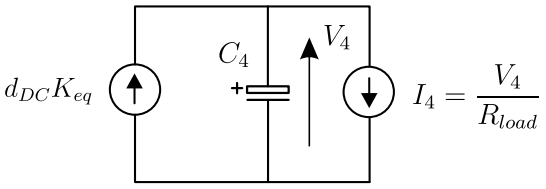

Fig. 5: Simplified model for the voltage control of the DC bus.

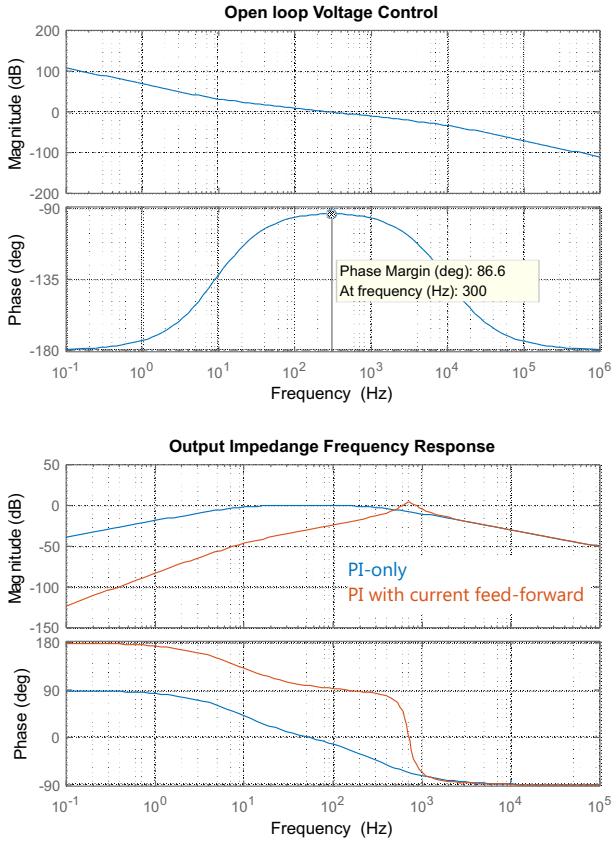

Fig. 6: Frequency response of the voltage control and of the output impedance.

intrinsically asymmetrical, i.e., the preferred power transfer direction is between the storage ports and the bus ports, a different mix of inductors can be chosen to reach the same equivalent inductor. In fact, the bus port could have a smaller inductor value than the other ports. This may be beneficial for optimization purpose, in fact the inductor connected to the bus port carries more current than the other. The design margin for the phase shift allows handing eventual design mismatches. A value of 500 uF is chosen for the output capacitance of each port. Table I summarizes the parameters of the simulations.

V_n (V_1, V_2, V_3, V_4)	28 V
P_n	2.5 kW
L_{lk} (L_1, L_2, L_3, L_4)	1 uH
L_{eq}	1.25 uH
C_1, C_2, C_3, C_4	0.5 mF
$C_{supercap}$	10 mF
$f_{3dB-bus}$	300 Hz
$f_{3dB-supercap}$	1 Hz
f_{sw}	20 kHz
f_{LPF}	1 Hz
f_{HPF}	5 Hz

TABLE I: Parameters for the simulations

In the simulations, the battery current reference is set to 3 A as an example. The capacitance of the supercapacitors is 10 mF. A purposely small value for the supercapacitor is chosen to show some remarkable voltage variation even with short simulation times. This condition emulates a request that cannot be satisfied by the fuel cells alone and where the energy storage system is required to provide the missing power. For simplicity, the battery and the fuel cell are modeled as ideal voltage sources, while resistors and controlled current sources simulate the loads at the bus. The QAB operates in voltage control mode, as described in Section IV. A voltage control bandwidth of 300 Hz is chosen for the bus regulator, while a very slow controller (1 Hz) was chosen for the supercapacitors. Choosing a slow controller ensures that there is not interaction between the other controls. Moreover, a voltage-dependent dynamic saturation of the phase shift of the supercapacitor port prevents its voltage to decrease or increase too much. In the case of saturation, the remaining power request is shifted from the supercapacitors to the batteries.

Fig. 7 shows a rapid change in the power consumption of

the bus. The voltages and currents at each port are reported, as well as the phase shift. In Fig. 7a a current step of 10 A happens at t = 0.5 s. Since there is no feed-forward, the bandwidth of the controller determines the voltage restoration. Moreover, due to the slow dynamic, the supercapacitors are not providing the major share of the current, like it is expected. Fig. 7b shows the same transient with the feed-forward enabled. However, a static-gain decoupling is implemented. Differently from the previous case, the voltage regulation is improved, and almost no undervoltage appears. The currents show that the supercapacitors are supplying the current for the transient. Fig. 7c shows the effect of the dynamic decoupling. The effect of the dynamic decoupling is to modify the phase shift taking into account the voltage difference. Since it is expected that the supercapacitors will discharge, the phase shift is incremented to provide more power. In fact, a slightly deeper discharge of 2 V is visible. To sum up, for voltage difference up to 25 %, the static decoupling still allows excellent tracking performance.

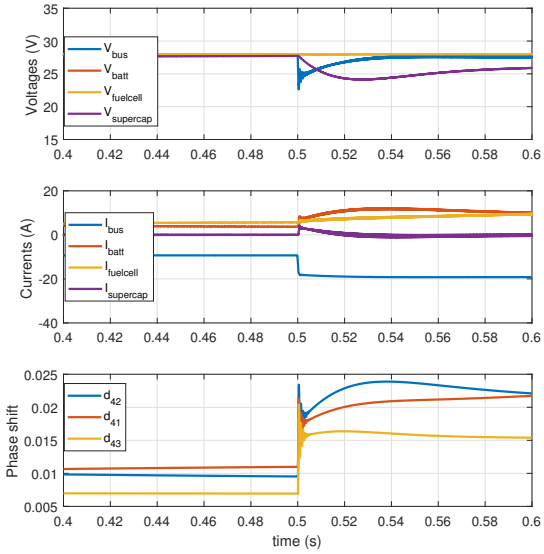

(a) Without current feed-forward and real-time decoupling

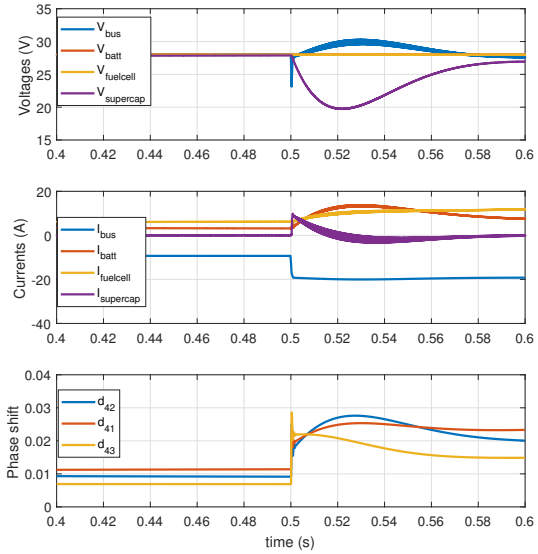

(b) With current feed-forward and with fixed decoupling.

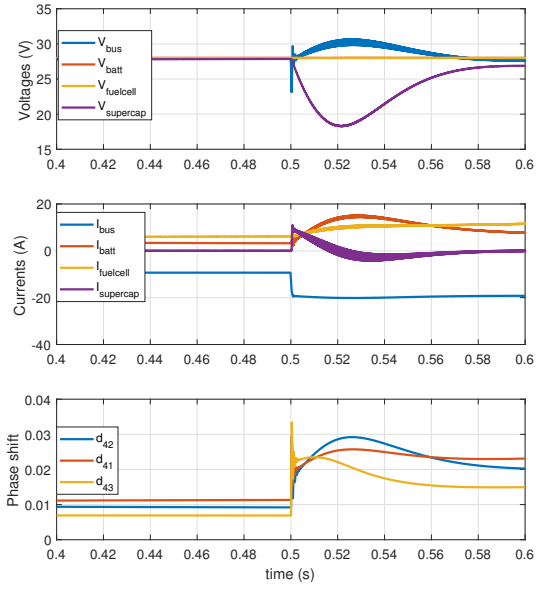

(c) With current feed-forward and real-time decoupling

Fig. 7: Simulation results of the QAB with a load step and different control strategies.

VI. Experimental Results

The goal of the experiments is to show a demonstrator for the HV 270 V application, as well as to show that the proposed control allows to properly regulate the power transfer between different ports. The focus is to highlight that the asymmetric operation of the converter does not cause an excessive efficiency drop.

A prototype of the QAB was used to test the proposed control. SiC components (Wolfspeed C2M0025120D) were employed and a high efficiency has been demonstrated in previous publications [13]. Considering the available equipment, the design is carried out at a reduced power, P_n = 3 kW. The nominal phase shift d_n = 0.1, leading to a needed inductance value of about 95 uH. As anticipated in the simulation results section, there is the degree of freedom to distribute the inductance between storage and bus ports, in this case a value of 160 uH was chosen for the storage ports and a smaller inductance (35 uH) was chosen for the bus port. Considering the leakage inductance of the transformer, the design value is reached. The transformer already showed

asymmetries of 10 % of the leakage inductance because of the different winding of the bus port, so keeping the symmetry would not have brought any advantage. The devices are chosen for availability reasons and are overdesigned for the demonstrator. In particular, considering 270 V nominal voltage (with 350 maximum operating voltage considering the MIL-STD), devices with breakdown voltage of 650 V could have been chosen. However, SiC devices manufactured have invested resources in optimizing the 1.2 kV devices for market reasons, as a consequence devices with better characteristics in this voltage range can be found. Having devices with higher breakdown voltage rating could also benefit the cosmic rays immunity, especially important at higher altitudes. Table II lists the parameters of the experimental results.

Fig. 8a shows a picture of the experimental setup, where the storage ports are connected to power supplies and the bus is emulated with electronic loads. It is assumed that all ports operate at the same DC voltage level for demonstration purpose. As a simplification, the decoupling is implemented with a constant matrix (the voltage variations are not taken into account).

Fig. 8 shows the results, in particular, Fig. 8b show the DC currents and the bus voltage in response to a load reduction. The port emulating the supercapacitors is providing the initial current peak, while the fuel cell shows a slow variation. This is in good agreement with the simulation of Fig. 7b: although the static decoupling is used, the performance is still very good.

V_n (V_1, V_2, V_3, V_4)	270 V
P_n	3 kW
L_1, L_2, L_3	160 uH
L_4	35 uH
L_{eq}	95 uH
C_1, C_2, C_3, C_4	0.4 mF
$f_{3dB-bus}$	100 Hz
f_{sw}	20 kHz

TABLE II: Experimental parameters

Fig. 8c shows the steady-state high-frequency waveforms for the QAB. As can be seen, the port emulating the fuel cell is providing the vast majority of the current, while the current of the other ports is reduced. The residual active power processed by the other ports (that should be zero in steady state) depends on the non-perfect compensation of the coupling. The outer voltage and SOC control would compensate for this effect in a real application.

The efficiency of the demonstrator was experimentally measured with the power meter Yokogawa WT1800. Two sets of measurements were performed: a first set where all three storage ports transfer power to the bus and a reduced set where only one storage port is transferring power to the bus. During this second test the other two storage ports are still switching and commutating with very low current. This represent the standard case where the fuel cell is providing the bulk power and the other storage are inactive. It also represents the most asymmetrical and challenging case, for this reason it was chosen to be measured. As can be seen, because of the

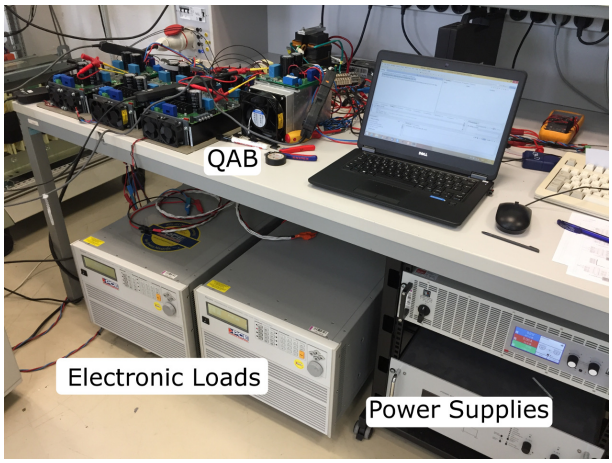

(a) Picture of the experimental setup.

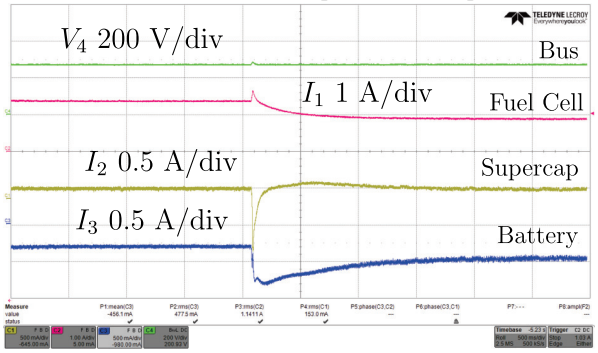

(b) Transient during load reduction.

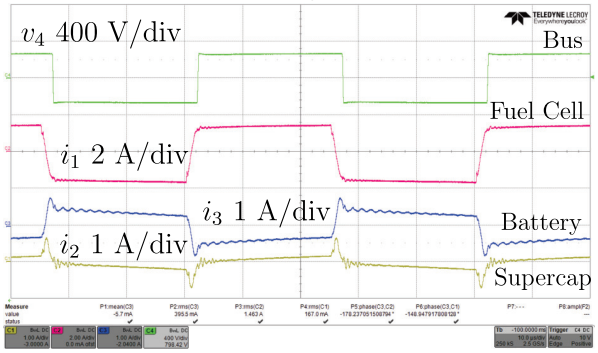

(c) Steady-state.

Fig. 8: Experimental results

soft-switching operation as well as the reduced current that is flowing in the ports that are not transferring power, only a small efficiency deterioration of 0.1 % at 2 kW happens.

VII. Conclusion

In this paper it has been demonstrated that the QAB converter can effectively be used as a storage manager for the More Electric Aircraft, guaranteeing the galavanic isolation between the ports and prioritizing the energy consumption from the fast energy sources. The main challenge is to control the power flow between different sources in a highly coupled structure of the QAB. The contribution of the paper is a novel

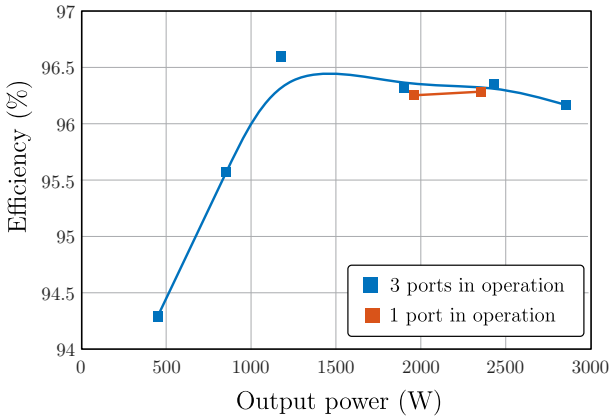

Fig. 9: Efficiency measurement of the QAB converter.

decoupling control plus a feed forward action, that allows controlling the power flow regardless the controller bandwidth.

Simulations showed that the feed-forward effectively increases the utilization of the supercapacitors as a fast energy source, while the dynamic decoupling further improves the performance. Experiments carried out in a HV scenario shows that the converter can achieve a very good efficiency with the use of SiC devices and the efficiency deterioration due to asymmetrical operation is 0.1 % at 2 kW. This means that the QAB can effectively substitute three single-input single-output power converters for the storage integration.

REFERENCES

[1] D. Barater, G. Buticchi, A. Soldati, G. Franceschini, F. Immovilli, M. Galea, and C. Gerada, "Multistress characterization of insulation aging mechanisms in aerospace electric actuators," in *2015 IEEE Energy Conversion Congress and Exposition (ECCE)*, Sept 2015, pp. 2215–2222.

[8] J. L. Duarte, M. Hendrix, and M. G. Simoes, "Three-port bidirectional converter for hybrid fuel cell systems," *IEEE Transactions on Power Electronics*, vol. 22, no. 2, pp. 480–487, March 2007.

[2] P. Wheeler and S. Bozhko, "The more electric aircraft: Technology and challenges." *IEEE Electrification Magazine*, vol. 2, no. 4, pp. 6–12, Dec 2014.

[3] L. Rubino, D. Iannuzzi, G. Rubino, M. Coppola, and P. Marino, "Concept of energy management for advanced smart-grid power distribution system in aeronautical application," in *2016 International Conference on Electrical Systems for Aircraft, Railway, Ship Propulsion and Road Vehicles International Transportation Electrification Conference (ESARS-ITEC)*, Nov 2016, pp. 1–6.

[4] M. Rashed, J. M. L. Peuvedic, and S. Bozhko, "Conceptual design of battery energy storage for aircraft hybrid propulsion system," in *2016 International Conference on Electrical Systems for Aircraft, Railway, Ship Propulsion and Road Vehicles International Transportation Electrification Conference (ESARS-ITEC)*, Nov 2016, pp. 1–6.

[5] S. Alahakoon and M. Leksell, "Emerging energy storage solutions for transportation a review: An insight into road, rail, sea and air transportation applications," in *2015 International Conference on Electrical Systems for Aircraft, Railway, Ship Propulsion and Road Vehicles (ESARS)*, March 2015, pp. 1–6.

[6] D. Salomonsson and A. Sannino, "Low-voltage dc distribution system for commercial power systems with sensitive electronic loads," *IEEE Transactions on Power Delivery*, vol. 22, no. 3, pp. 1620–1627, July 2007.

[7] H. Tao, A. Kotsopoulos, J. L. Duarte, and M. A. M. Hendrix, "Family of multiport bidirectional dc-dc converters," *IEE Proceedings - Electric Power Applications*, vol. 153, no. 3, pp. 451–458, May 2006.

[9] S. Falcones, R. Ayyanar, and X. Mao, "A dc-dc multiport-converter-based solid-state transformer integrating distributed generation and storage," *IEEE Transactions on Power Electronics*, vol. 28, no. 5, pp. 2192–2203, May 2013.

[10] R. Teodorescu, M. Liserre, and P. Rodriguez, *Grid Converters for Photovoltaic and Wind Power Systems*. Wiley, Jan 2011.

[11] L. Cao, K. H. Loo, and Y. M. Lai, "Output-impedance shaping of bidirectional dab dc-dc converter using double-proportional-integral feedback for near-ripple-free dc bus voltage regulation in renewable energy systems," *IEEE Transactions on Power Electronics*, vol. 31, no. 3, pp. 2187–2199, March 2016.

[12] G. Buticchi, M. Andresen, M. Wutti, and M. Liserre, "Lifetime-based power routing of a quadruple active bridge dc/dc converter," *IEEE Transactions on Power Electronics*, vol. 32, no. 11, pp. 8892–8903, Nov 2017.

[13] G. Buticchi, L. Costa, and M. Liserre, "Improving system efficiency for the more electric aircraft: A look at dcdc converters for the avionic onboard dc microgrid," *IEEE Industrial Electronics Magazine*, vol. 11, no. 3, pp. 26–36, Sept 2017.